2021 IEEE Nuclear Science Symposium and Medical Imaging Conference (NSS/MIC) | 978-1-6654-2113-3/21/$31.00 ©2021 IEEE | DOI: 10.1109/NSS/MIC44867.2021.9875861

Simulation Study of a Non-Human Primate PET System Based on a DOI-Capability Detector Block

Li Cheng, Mengle Xue, Yingcai Ji, Shuai Huang, Nianming Jiang, Yaqiang Liu*

***Abstract*–In this work, a half-meter-long PET scanner was designed based on a 7mm-DOI-capability detector block to achieve both high spatial resolution and high sensitivity for non-human primate (NHP) imaging. The scanner consists of 15 block rings in axial and 36 blocks per ring. The performance of the proposed design was evaluated based on GATE simulations. The sensitivity at the center of field-of-view (FOV) was 19.3% with a 250~750 keV energy window. A mini-Derenzo phantom study demonstrated that 1.0 mm hot rods could be recovered at the FOV center, while 1.4 mm hot rods could be partially identified near the edge of 30 cm transverse FOV. NCAT phantom was zoomed out and simulated to evaluate the imaging performance of short frame time. Besides, we compared the proposed design with the mini-EXPLORER II PET scanner by calculating Cramer-Rao lower bound. The result demonstrated that although lack of TOF capability, the proposed design performed better at larger radial offset (>~6 cm) in the transverse plane, and it also outperformed in the axial direction because it suffered less from axial parallax error and the compact design led to higher sensitivity.**

I. Introduction

Positron Emission Tomography (PET) is an advanced molecular imaging technique and plays an important role in current biomedical research. However, different from small animal imaging, which can be performed in dedicated PET scanners for better performance, non-human primates, such as rhesus monkeys, are usually scanned on human scanners. Therefore, to optimize the imaging performance, a dedicated primate PET scanner needs to be designed.

For a primate PET scanner, high spatial resolution and high sensitivity are required to better visualize *in vivo* tracer distribution. As a part of the EXPLORER project, mini-EXPLORER II[1] system achieves excellent performance for primates imaging. However, due to the lack of depth-of-interaction (DOI) information, the image quality will suffer from the parallax error in both transverse and axial directions. Besides, mini-EXPLORER II is relatively larger and too expensive.

Manuscript received December 3, 2021.

Li Cheng is with the Key Laboratory of Particle & Radiation Imaging, Ministry of Education and Department of Engineering Physics, Tsinghua University, Beijing, 100084, China. (E-mail: chengli.thu10@gmail.com).

Yaqiang Liu (Corresponding author) is with the Key Laboratory of Particle & Radiation Imaging, Ministry of Education and Department of Engineering Physics, Tsinghua University, Beijing, 100084, China. (E-mail: liuyaqiang@mail.tsinghua.edu.cn).

Mengle Xue, Yingcai Ji, Shuai Huang, Nianming Jiang are with the Beijing Novel Medical Equipment Ltd, Beijing, 102206, China.

In this paper, we propose a compact design of a primate PET scanner based on a DOI detector block[2] to achieve better imaging performance and reduce commercial cost. Sensitivity and spatial resolution were evaluated based on GATE simulation. NCAT phantom was employed to evaluate the short-time imaging performance of the scanner. In addition, Cramer-Rao lower bound was computed to compare the performance of the proposed design and mini-EXPLORER II.

II. Materials and Methods

A. System Design

This work is based on an available detector block with depth-of-interaction (DOI) capability (Fig. 1). Its energy resolution is 12.6%. We propose to build a half-meter-long scanner that can cover almost all interested organs of non-human primates and achieve high sensitivity. Details about the detector block and the system geometry are shown in Table I and Fig. 2.

Compared with the proposed design, the mini-EXPLORER II scanner uses a larger crystal (2.76×2.76×18.1 mm^3) and does not have DOI capability. Its ring diameter and axial FOV are 520 mm and 483 mm respectively. In total, ~13000 mL LYSO crystals were used to build the system. Besides, its TOF resolution can achieve 410 ps.

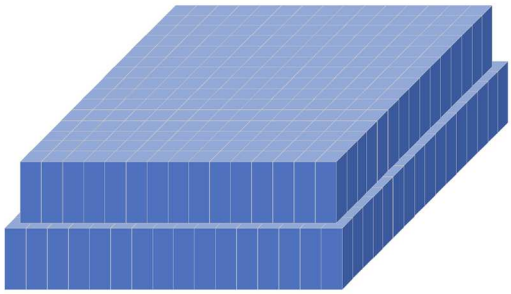

Fig. 1. A dual-layer-offset detector block. Top layer: 15 × 15 LYSO crystals, bottom layer: 16×16 LYSO crystals.

TABLE I. System Configuration of the Proposed PET Scanner

System Parameters	Description
Crystal Size	2.0×2.0×7.0 mm^3
Crystal pitch	2.1 mm
Block pitch	33.8 mm (transaxial) × 33.9 (axial) mm
Block Number Per Module	2 (transaxial) × 3 (axial)
Module Number	18 (transaxial) × 5 (axial)
Total crystal volume	7273 mL

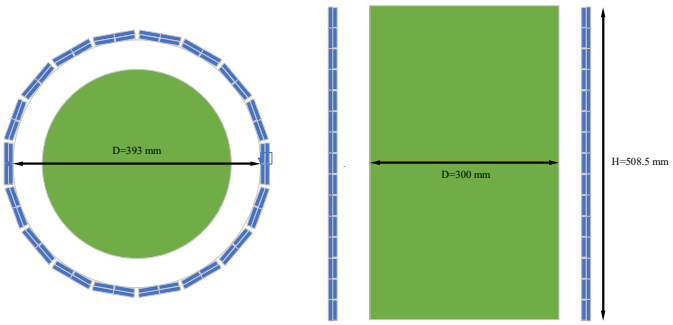

Fig. 2. Geometry of the proposed scanner. The target FOV is 300 mm.

B. Performance evaluation

Monte Carlo simulations based on GATE v8.0 were used to evaluate the performance of the proposed system, including system sensitivity, spatial resolution and short time imaging performance. Besides, Cramer-Rao lower bound was computed to compare the quantification performance of 2 different designs. A GPU-accelerated list mode reconstruction was employed for image reconstruction, and it was implemented on a computer with NVIDIA RTX 2080 Ti. 10 subsets and 10 iterations were used for all reconstructions.

1) System sensitivity

A point Fluorine-18 source surrounded by a 1-mm-radius water sphere was placed at the center of FOV, and 10 million annihilations were simulated in total. System sensitivity was calculated with 2 different energy window settings: 250~750 keV and 450~650 keV, which are common options for small animal imaging and human imaging, respectively.

2) Spatial resolution

A mini-Derenzo phantom filled with Fluorine-18 source was placed at the center (r=0 mm) and edge (r=130 mm) of FOV. A water cylinder phantom, whose diameter was 40 mm, was simulated for attenuation. For each case, 243 million annihilations were simulated.

3) Short time imaging performance

A 3D NCAT phantom was zoomed out for evaluation. It was digitized with a 2.0×2.0×1.05 mm^3 voxel size and the image matrix size was 149×149×97. In total, 584.0 million annihilations were simulated, equivalent to 1.57 mCi injection and 10 s scan.

4) Cramer-Rao lower bound

Cramer-Rao (CR) bound, which is the lower bound on the variance of an unbiased estimator, was employed to compare the quantification performance of 2 different system designs. For a selected region-of-interest (ROI), its CR bound V_{CR} can be computed according to (1), where $\boldsymbol{f}$ is the indicator function of ROI and $\boldsymbol{F}$ is the Fisher information matrix, which is calculated by (2). $\boldsymbol{P}$ is the system matrix, $\bar{\boldsymbol{y}} = \boldsymbol{Px}$ is the expectation of the PET data and $\boldsymbol{x}$ is the activity distribution image.

$$V_{CR} = \boldsymbol{f}'\boldsymbol{F}^{-1}\boldsymbol{f} \quad (1)$$

$$\boldsymbol{F} = \boldsymbol{P}'[\tfrac{1}{\bar{\boldsymbol{y}}}]\boldsymbol{P} \quad (2)$$

When modeling the system matrix, each crystal was divided into multiple sub-crystals and $\boldsymbol{P}$ was calculated using numerical integration[3]. The solid angle effect and photon penetration effect inside crystals were both considered. The calculated system matrix was corrected by a global factor to match the true sensitivity at the FOV center, which was estimated from the GATE simulation. TOF capability was considered when calculating the system matrix for mini-EXPLORER II. As shown in Fig. 3, both transverse and axial performance were evaluated.

To demonstrate the effect in the transverse plane, we simulated one block ring of our proposed design and two block rings of the mini-EXPLORER II scanner, corresponding to similar axial lengths (33.9 mm & 34.3 mm). A uniform water cylinder with a diameter of 280 mm was digitized with a 2×2×35 mm^3 voxel, and the image matrix size is 149×149×1.

Similarly, we picked up a uniform phantom, which was digitized by a 1×1×223 image matrix array with a 10×10×2.1 mm^3 voxel size. And we calculated the CR bound of these voxels to demonstrate the performance in the axial direction.

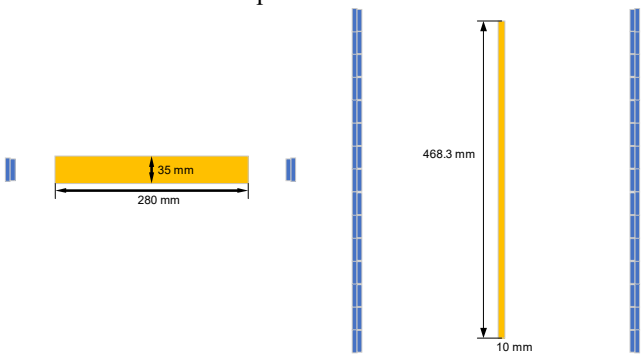

Fig. 3. Illustration of CR bound evaluation in transverse (a) and axial (b) direction.

III. RESULTS

A. Sensitivity and spatial resolution

There are no reference energy window settings for primate imaging, system sensitivity for different energy window options is listed in Table II. F-18 branching ratio and attenuation effect were ignored. The system sensitivity is much higher than most commercial systems which are designed for human imaging. If not specified, a 250~750 keV energy window is employed in other studies in this work.

TABLE II. SYSTEM SENSITIVITY AT FOV CENTER

Energy window	sensitivity
250~750 keV	19.3%
450~650 keV	14.1%

Fig. 4 shows the reconstructed images of the mini-Derenzo phantom at the center (r=0 mm) and edge (r=130 mm) of FOV. At the center of FOV, 1 mm hot rods can be identified. However, at the edge of FOV, due to the parallax error effect, hot rods whose diameter is less than 1.4 mm can't be recovered and 1.4 mm hot rods can be partially identified.

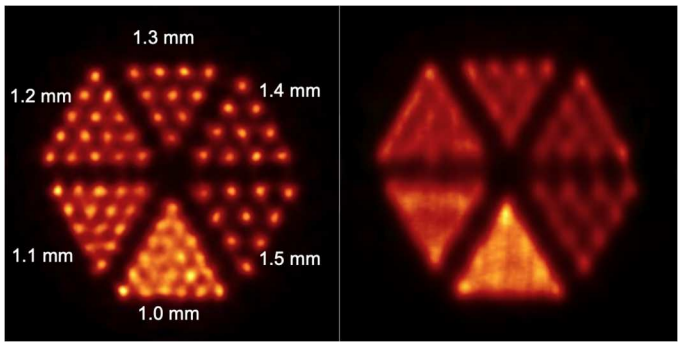

Fig. 4. Reconstructed images of mini-Derenzo phantom at r=0 mm (left) and r=130 mm (right). The image pixel size is 0.25 mm in transverse plane.

B. NCAT phantom study

Fig. 5 shows the true and reconstructed activity distribution in the NCAT phantom. With 1.57 mCi injection, 64.5 million true coincidences were collected even though the scan time was only 10 s. Two lesions in the lung region can be identified because of the high sensitivity and resolution. Besides, due to relatively lower contrast and higher background noise, the lesion in the liver region is not very clear, but can still be identified. This result demonstrates the potential advantage of the proposed scanner in dynamic imaging.

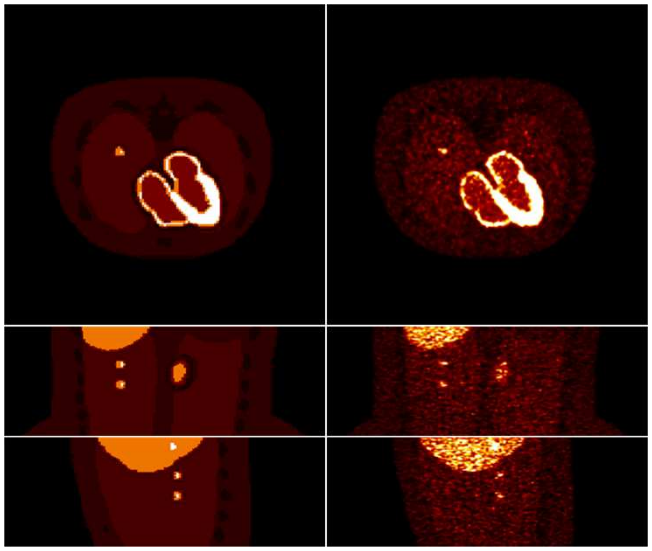

Fig. 5. True activity distribution (left) and reconstructed images (right). From top to bottom are transverse, coronal and sagittal slices.

C. CR bound evaluation

In Fig. 6 and Fig. 7, we compare the CR bound performance of the proposed design and mini-EXPLORER II. Benefiting from TOF information, CR bound of mini-EXPLORER II is lower than that of the proposed design at the FOV center in the transverse plane, as shown in Fig. 6. However, at large radial offsets (r>~60 mm), where parallax error rather than TOF benefit is more significant, the proposed design with DOI capability outperforms mini-EXPLORER II.

Fig. 7 demonstrates the performance of ROI quantification in the axial direction. Compact design leads to higher sensitivity, thus the CR bound of the proposed design is relatively lower. By comparing (a), (b) in Fig. 6 and Fig. 7, it's clear that the performance of the proposed system is much better in smaller ROI quantification, which can be explained by better spatial resolution determined by smaller crystal size and DOI information.

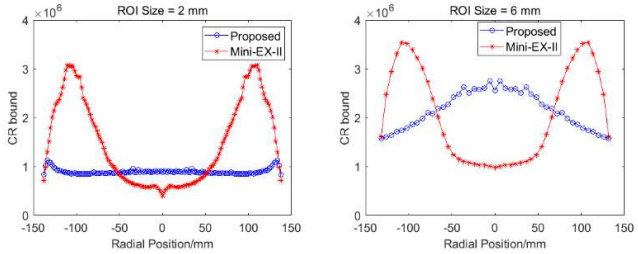

Fig. 6. Plots of the CR bounds for different ROI size at different radial positions.

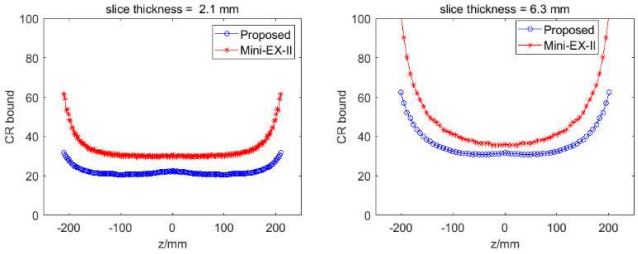

Fig. 7. Plots of the CR bounds for different slice thickness at different axial positions.

IV. SUMMARY

In this study, we propose a more cost-effective primate PET scanner, which uses only 56% crystals of mini-EXPLORER II. The performance of the proposed design was evaluated by simulation studies. Preliminary results indicate that the proposed design can achieve high sensitivity (~19.3% at the FOV center, with a 250~750 keV energy window), and high and relatively uniform spatial resolution (1.0 mm at the center and 1.4 mm near FOV edge). Furthermore, the NCAT phantom study demonstrates the potential for better dynamic imaging with a short frame time. At last, comparison with mini-EXPLORER II demonstrates the advantage of DOI capability and better spatial resolution for a long PET scanner. Due to its excellent performance, the proposed system will be a powerful tool for primates-based biomedical research. And its performance is expected to be further improved after incorporating TOF information.

V. REFERENCES

[1] Y. Lyu, X. Lv, W. Liu, M. S. Judenhofer, A. Zwingenberger, E. Wisner, *et al.*, "Mini EXPLORER II: a prototype high-sensitivity PET/CT scanner for companion animal whole body and human brain scanning," *Physics in Medicine and Biology,* 2019.

[2] Q. Wei, T. Xu, T. Dai, S. Wang, Y. Liu, Y. Gu, *et al.*, "Development of a compact DOI–TOF detector module for high-performance PET systems," *Nuclear Science and Techniques,* vol. 28, no. 4, p. 43, 2017.

[3] R. H. Huesman, G. J. Klein, W. W. Moses, J. Qi, B. W. Reutter, and P. R. Virador, "List-mode maximum-likelihood reconstruction applied to positron emission mammography (PEM) with irregular sampling," *Medical Imaging IEEE Transactions on,* vol. 19, no. 5, pp. 532-537, 2000.